Failure Mechanisms and Color Stability in Light-Emitting Diodes during Operation in High-Temperature Environments in Presence of Contamination

Pradeep Lall[(1)], Hao Zhang[(1)], Lynn Davis[(2)]
[(1)] Auburn University
NSF-CAVE3 Electronics Research Center
Department of Mechanical Engineering
Auburn, AL 36849
[(2)] RTI International, Research Triangle Park, NC 27709
Tele: 334-844-3424
E-mail: lall@auburn.edu

Abstract
The energy efficiency of light-emitting diode (LED) technology compared to incandescent light bulbs has triggered an increased focus on solid state luminaries for a variety of lighting applications. Solid-state lighting (SSL) utilizes LEDs, for illumination through the process of electroluminescence instead of heating a wire filament as seen with traditional lighting. The fundamental differences in the construction of LED and the incandescent lamp results in different failure modes including lumen degradation, chromaticity shift and drift in the correlated color temperature. The use of LED-based products for safety-critical and harsh environment applications necessitates the characterization of the failure mechanisms and modes. In this paper, failure mechanisms and color stability has been studied for commercially available vertical structured thin film LED (VLED) under harsh environment conditions with and without the presence of contaminants. The VLED used for the study was mounted on a ceramic starboard in order to connect it to the current source. Contamination sources studied include operation in the vicinity of vulcanized rubber and adhesive epoxies in the presence of temperature and humidity. Performance of the VLEDs has been quantified using the measured luminous flux and color shift of the VLEDs subjected to both thermal and humidity stresses under a forward current bias of 350 mA. Results indicate that contamination can result in pre-mature luminous flux degradation and color shift in LEDs.

Introduction
Over the last few decades, LEDs have become one of the mainstream illumination sources due to their advantages in energy efficiency, long lifetimes, and environmental friendliness. Among the various types of LEDs, InGaN based LEDs have been the most widely used for SSL devices. They can be seen in numerous lighting applications because of their high current injection efficiency and blue-light emission [Schubert 2006, Kim 2007]. InGaN LEDs, along with a yellow phosphor layer, is the preferred method to produce artificial white light. The yellow phosphor can be placed directly or remotely in relation to the LED to produce a spectral power distribution (SPD) of what is perceived as white light. Currently, phosphor converted LEDs (pc-LEDs) use phosphor constructed of a garnet that has been doped with a heavy earth metal place directly on the LED. The most commonly used phosphor is cerium (Ce^{3+}) doped Yttrium aluminum garnet (Ce-YAG, Y3AL5O12) [Qin 2011; Ye 2010; van Driel 2011]. The phosphor particles are spin coated with a binder, such as silicone, in order to directly attach to the LED. The unique silicone polymer utilized in pc-LEDs is stable over a wide temperature range and resistant to yellowing after ultraviolet exposure. Furthermore, silicone can be formulated with different hardness properties, which can be either a gel, an elastic solid, or a more rigid material. Silicone used in LED encapsulation is generally elastic, which gives the needed flexibility to encapsulate the wirebond and LED die. Additionally, this characteristic provides the ability to absorb thermal stress from the soldering process and during high power operations.

Previous researchers have shown that LEDs rarely fail catastrophically; instead, their light output degrades slowly over time. Generally, there are two predominate degradation mechanisms. One mechanism is the degradation of the LED chip due to the increase of non-radiative recombination which reduces the total number of emitted photons [Rossi 2006; Tomiya 2004; Lee 2008]. The other predominant mechanism is the degradation of the optical parts under temperature or electric stresses [Narendran 2004; Chang 2012; Pavesi 2004; Meneghesso 2003; Hoang 2005; Hong 2005]. If an LED is in the presence of VOCs, then VOCs can diffuse into the gas-permeable silicone lens and encapsulants. The VOCs will occupy the free space in the molecular structure of the silicone. Once exposed to high photonic energy emitted by the LED and heat from the junction temperature, the VOCs start to discolor and deteriorate the pc-LED [Rossi 2006]. The predominant failure mechanism of VOC contamination is the discoloration of the phosphor layer. After VOC contamination occurs, the degradation of luminous flux and the chromaticity shift becomes extremely rapid. Several LED manufacturers have released application notes pertaining to the chemical compatibilities of the LED products [Cree 2013; Samsung 2013]. Material selection considerations and chemical compatibility test methods are outlined in order to increase the overall lifetime of LEDs through the reduction of VOCs during operation. However, no detailed failure analysis of VOCs contamination and reversibility has been seen in literature which necessitates the investigation presented in this work.

In this paper, VLEDs from the same manufacturer have been studied in a contaminated and uncontaminated environment. Periodically, luminous flux and CCT were recorded in order to correlate the photometric and colorimetric results to the predominant failure mechanisms previously described. The lighting measurements followed the LM-79-08 test standard [2008]. In addition, the VLEDs were subject to a steady-state temperature humidity life test of 85/85 with an

electrical bias based on the JEDEC standard JESD22-A101C [2009] and other reports [Davis 2013, 2014]. Upon completion of the accelerated testing, a pristine sample and the contaminated samples were cross-sectioned to further investigate the contamination area of the VLED package. From the cross-sectional analysis, it was observed that VOC contamination occurred in the phosphor binder layer only. The contamination process was found to be reversible when the contaminated samples were moved to a VOC free environment. The photometric results, as well as the failure analysis of the VLEDs are presented in this paper.

Experimental Setup

Test Samples

Several of the same LED product from the same manufacturer were used for experimental measurements throughout the experiment. Each LED consists of a blue emitting-LED chip covered by Yttrium aluminum garnet (YAG, Y3AL5O12) phosphor and silicone encapsulation. The yellow-based phosphor coating converts the blue light to a broader white light spectrum. The test samples can be powered with a constant current up to 1500mA. Figure 1 shows the samples used in the experiment. During the test, samples of the same LED package are separated into two groups. Each group had a population of five. The first group stayed in the contaminated chamber until complete failure. Samples of the second group had been moved into VOCs free chambers after the observation of VOC contamination to monitor the reversibility of contamination.

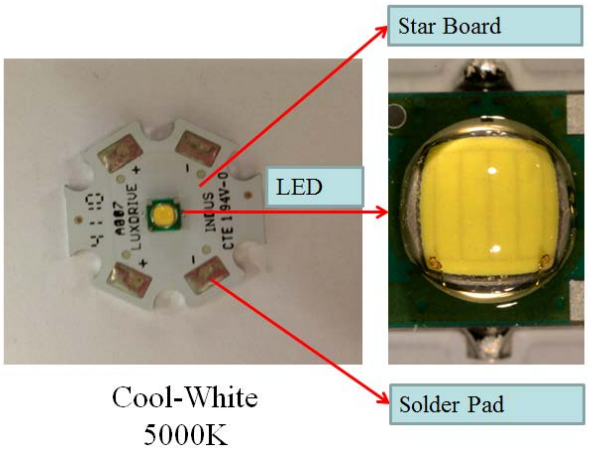

Figure 1. Test Sample

Contamination Sources

In this test two potential contamination sources have been studied. The first is the port stopper of the thermal and humidity chamber and it is made of vulcanized rubber. Sulfur is added to the natural rubber during the vulcanization process. However, sulfur is known to escape from the rubber, although with short chain plasticizing molecules at high temperature. The second potential source of contamination is the adhesive epoxy used in the thermal and humidity chamber. In order to fix the thermal couple and humidity sensor, a lot of adhesive epoxy were used in the chamber during the maintenance. After the test, an obvious discoloration of the adhesive epoxy can be observed. Figure 2 shows the contamination source for this experiment.

Figure 2. Potential Contamination Sources

Test Matrix

Figure 3 shows the heat sink and fixture used in this work for the environmental chamber. In this setup, a single LED was mounted on the top of a star board that was fixed on the top of the heat sink with screws and nylon insulation. The nylon insulation pad was used to prevent electric connection between the star board and the heat sink. Test samples were subjected to both thermal and relative humidity stress in a contaminated chamber. Figure 4 shows the thermal and humid chamber used in this experiment.

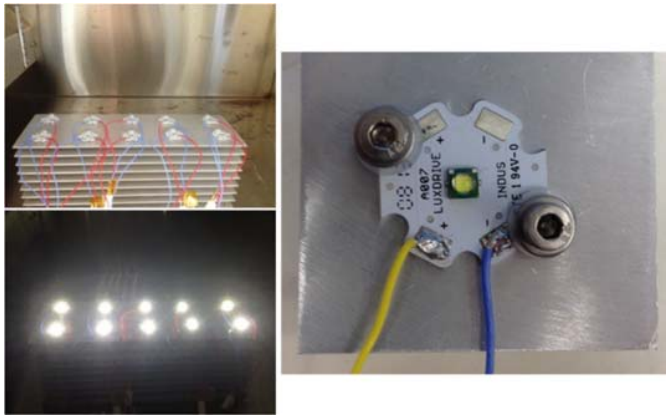

Figure 3. Test Setup

Figure 4. Temperature and Humidity Chamber

The accelerated test temperature was 85°C and the relative humidity was 85%. During the test, LED packages were power cycled at one-hour intervals. A constant current output driver outside of the chamber was utilized to power the LED packages at 350mA. The samples were examined at intervals of 168 hours (one week). Figure 5 shows the electric parameters used

in the experiment. At each measurement time, the LED packages were taken out of the chamber and cooled down to room temperature. After the test, the LEDs were attached to the heat sink again and moved back into the chamber. Thermal management is a key issue during the experiment. Without proper fastening of the star board and heat sink, the high junction temperature could cause the carbonization of the encapsulations.

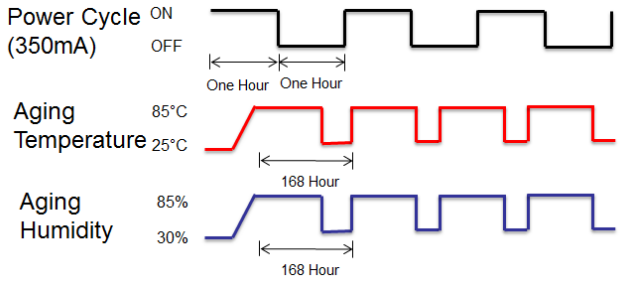

Figure 5. Electric parameters

Parameter Measurement

The LEDs were removed from the heat sink used in the environmental chamber and mounted on a fin heat sink in the integrating sphere, in order to perform photometric measurements. Luminous flux, chromaticity coordinate, and color temperature were recorded in the integrating sphere according to the LM-79-08 "Electrical and Photometric Measurement of Solid State Light Product" [2008], at each measurement time. During the test, LEDs were connected through the power cord inside the integrated sphere. A forward current of 1000 mA was used to acquire the photometric quantities of the test vehicles which were well below the maximum sustainable forward current of 1500 mA. The electrical bias used during the accelerated life test was 350 mA. Both current-levels were among the functional range according to the datasheet for the LED. In order to record the discoloration process under the contamination environment, pictures of the LED lens and phosphor were taken.

Luminous Flux Measurement was performed by utilizing an integrated sphere and a spectroradiometer. Air movement was minimized and the temperature inside the sphere was not subject to the ambient temperature outside of the sphere. A spectroradiometer was utilized to measure the radiant flux of the LEDs, from which luminous flux and chromaticity coordinates were calculated. Figure 6 shows the integrating sphere system which was used to measure the absolute radiant flux. 4π geometry was used in the radiant flux measurement. The testing sample can also be seen clearly in Figure 6.

Color Shift Distance is the absolute distance between the accelerated tested LED modules' chromaticity coordinates and the pristine LED modules' chromaticity coordinates in the CIE 1976 color space which is accepted by CIE in 1976 [23-24]. Monitoring the color shift path helps to understand which parts of a LED package fails. It can also be helpful for LED designers. Color Shift Distance calculation is given by:

$$\Delta u'v' = \sqrt{(u_i - u_o)^2 - (v_i - v_0)^2} \qquad (1)$$

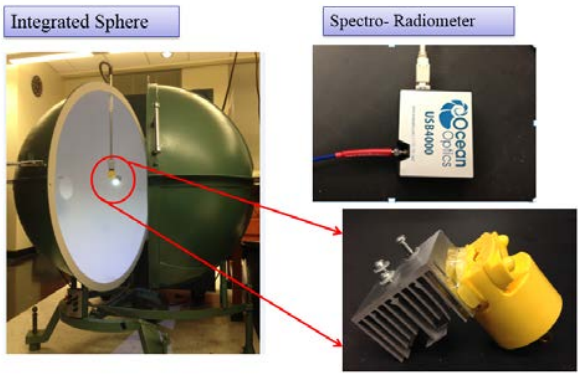

Figure 6. Integrating Sphere System

Test Results

For the first group in which the LEDs have been tested in an accelerated chamber with a port stopper made of vulcanized rubber, it is seen that the luminous flux of the LEDs degraded dramatically in a short time due to the VOC contamination. For the second group in which the contamination source is the adhesive epoxy used in accelerated chambers, it is seen that the VOC contamination process was reversible, if samples were transferred to a clean environment. During the test, pictures were taken to record the discoloration process at each readout time with digital camera. Figure 7 and Figure 8 show the expansion of the discolored area caused by VOCs contamination for the first group. The black area only appears in the phosphor layer. Detailed analysis of the phosphor layer is presented the subsequent sections of the paper.

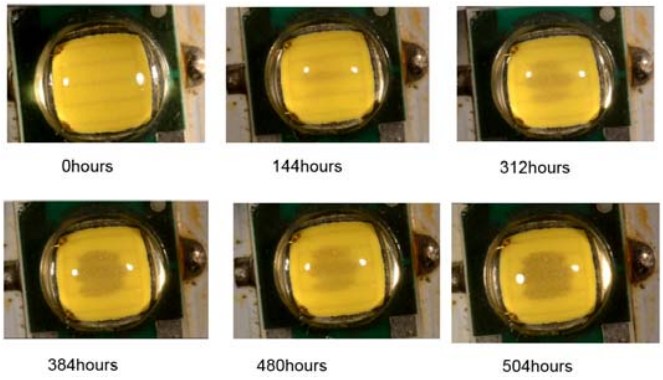

Figure 7. Sample 1of the First Group

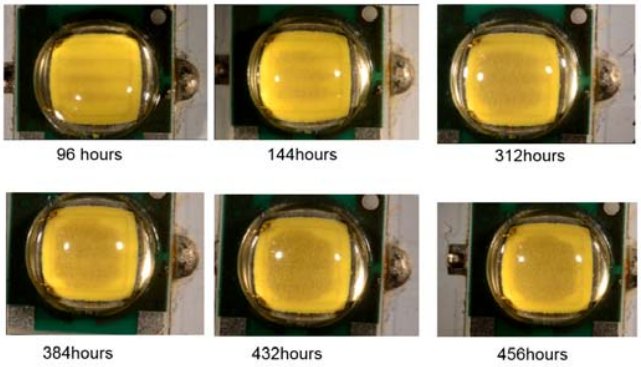

Figure 8. Sample2 of the First Group

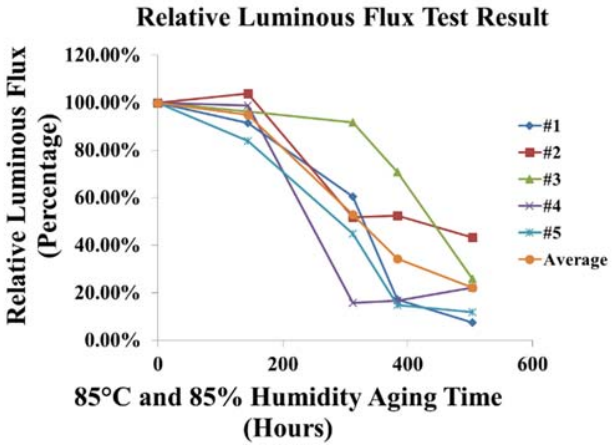

Figure 9. Luminous Flux of Group 1

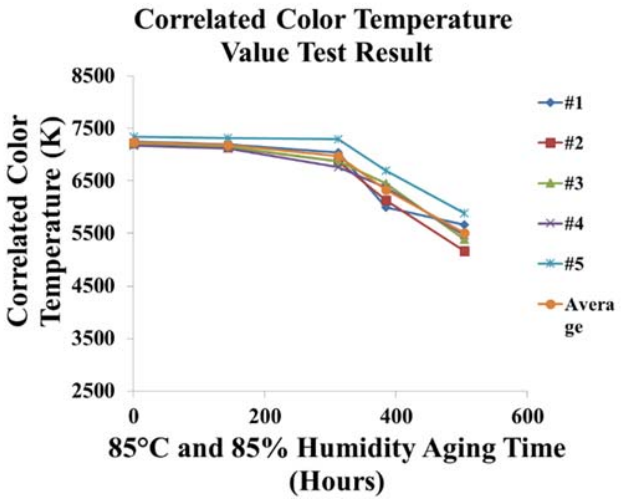

Figure 10. Correlated Color Temperature of Group 1

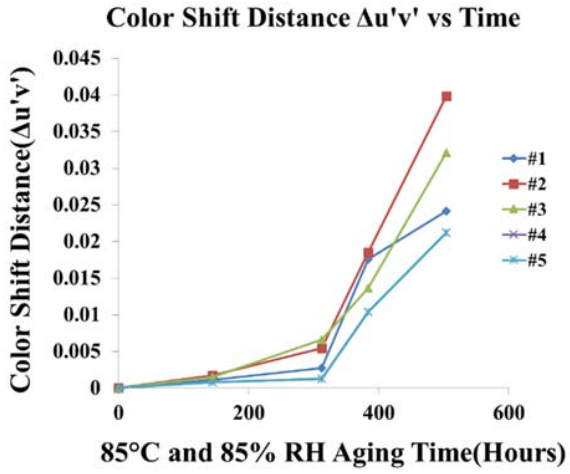

Figure 11. Color Shift Distance of Group 1

Figure 9 shows the relative luminous flux of the group1 samples during the test. It is obvious that the luminous flux drops dramatically in a very short time in conjunction with the appearance of discoloration area on the phosphor layer of the LED. In addition, because of the discoloration of the phosphor, the color temperature of the lamp shifts dramatically. Figure 10 shows the recorded data of correlated color temperature. The change in the correlated color temperature indicates that the color shifts from white color to yellow after exposure to contamination. Figure 11 shows the color shift distance of group 1 samples during the test in the u'v' space. In the contaminated chamber with a vulcanized rubber port stopper, it is seen that the color shifts dramatically in short time indicated by the increase in the Δu'v' values as a function of time. Figure 12 shows the color shift path of one sample from group1 in ANSI tolerance for SSL source in the 1976 u', v' chromaticity diagram [NEMA 2011; Judd 1936]. The color shift follows the black arrow in Figure 12. Following the arrow, the color shift from near the Planckian locus to yellow area indicates a filtering of blue emission.

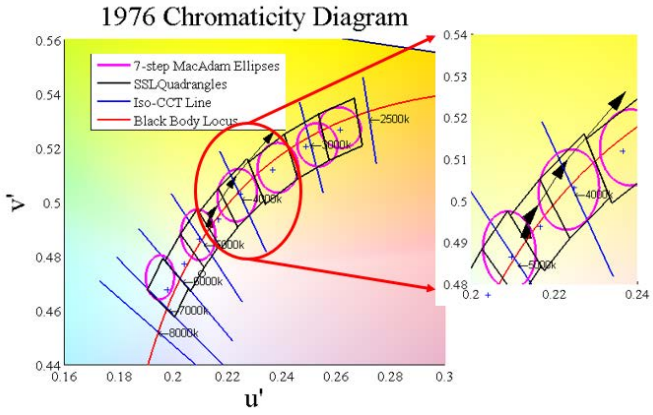

Figure 12. Color Shift in Chromaticity Tolerance of ANSI of Group 1

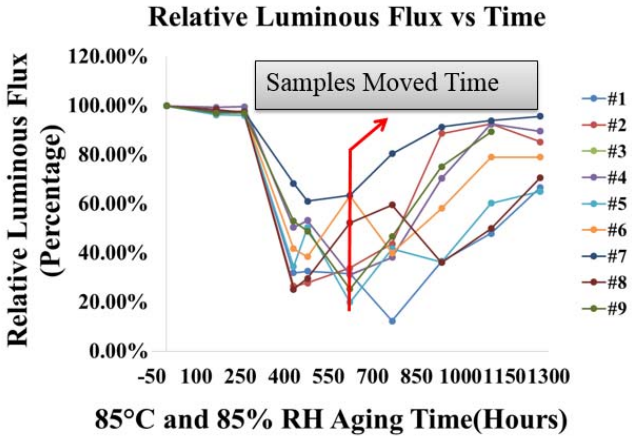

Figure 13. Relative Luminous Flux of Second Group

The second group with the adhesive epoxy contamination source exhibits a discoloration process that is reversible when samples were moved to VOCs free environment. Luminous flux output of the LED test samples increases again once the samples are moved to a contamination free environment. Furthermore, color coordinates in chromaticity space are found to shift back to location near white point. Figure 13 is the test result of relative luminous flux for the group2 samples. Relative luminous flux goes down dramatically caused by the

VOC contamination and then goes up when samples were transferred to clean chamber. Figure 14 shows the correlated color temperature test result of the second group. From the test result, the CCT value drops first and then starts to increase caused by the disappearance of discoloration area.

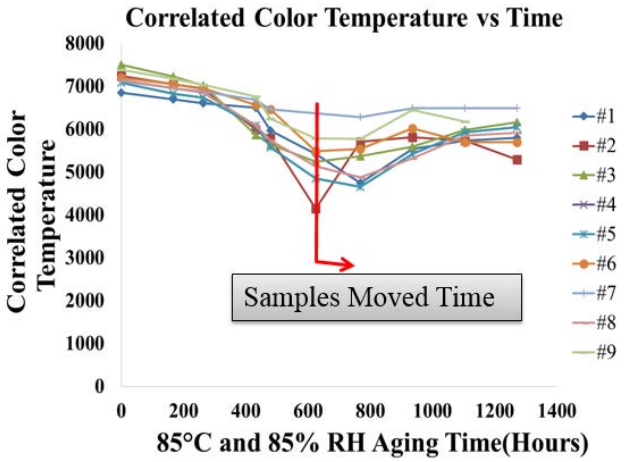

Figure 14. CCT Value of the Second Group

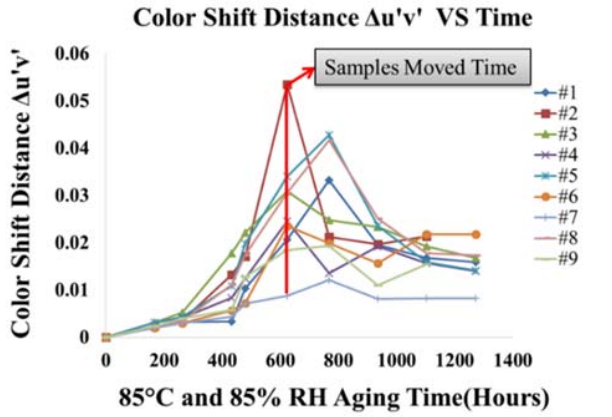

Figure 15. Color Shift Distance of the Second Group

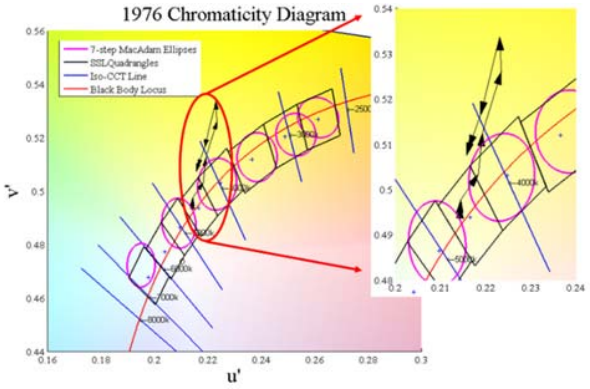

Figure 16. Color Shift in Chromaticity Tolerance of ANSI of Group 2

Figure 15 shows the color shift distance during the group2 test. In the contaminated chamber, color shift dramatically in short time. It is seen that when the samples were removed to clean chamber, the color shift distance starts to decrease, because of the disappearance of discoloration area. Figure 16 shows the color shift path of a sample from group 2 in ANSI tolerance for SSL source in the 1976 u', v' chromaticity diagram. The color shift follows the black arrow in Figure 16. Following the arrow, the color shifts from near the Planckian locus to the yellow area after contamination. However, when the samples were moved to VOCs free environment, the chromaticity coordinates of the LED migrate back to a location near the Planckian locus.

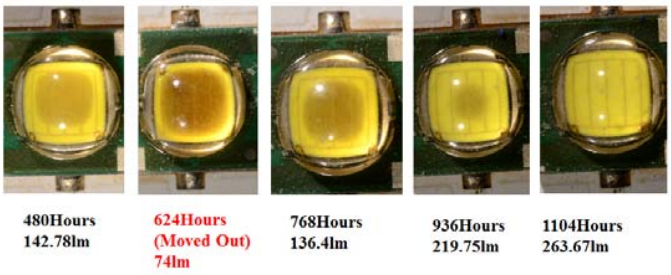

Figure 17. Sample1 of the Second Group

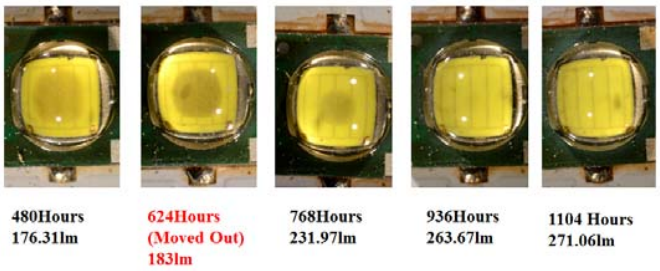

Figure 18. Sample2 of the Second Group

During the reverse process, optical image of LED package was recorded to monitor the change of the contamination area on the phosphor layer. From the following Figure 17 and Figure 18, it can be seen that VOC contamination is reversible when samples were moved to VOC free environment. After taking measurement for 624 hours in contaminated environment, samples were moved to VOC free environment. The black area on the phosphor is caused by the discoloration of VOCs. It was observed that the lens did not change during the experiment after exposure to environmental contaminants.

Discussion of the Failure Mechanisms

It is hypothesized that during the accelerated test, high temperature and high percentage relative humidity exposure caused the vulcanized rubber and epoxy start to release volatile organic compounds. Due to the sealed environment inside the accelerated test chamber, the high density of the VOCs diffused into the silicone polymer and were trapped into the space between the phosphor particles. When the LEDs went through the power cycle, high junction temperature and radiant power from the chip caused the trapped VOCs to produce discoloration of the phosphor. The discoloration of the phosphor caused the luminous flux to degrade dramatically and caused the color coordinates to shift significantly in the yellow direction. However, when the test samples were moved to a VOCs free environment, the VOCs trapped inside the phosphor particles diffused out causing the discoloration to disappear. The discoloration process caused by VOCs is reversible under

clean environment. Figure 19 shows the discoloration appearance of the VOCs contaminated LED. From the digital image, Discoloration occurs around the top surface of the LED chip because this is where the greatest heat and flux density comes into contact with the phosphor binder.

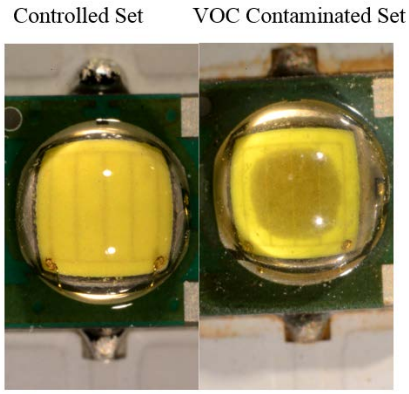

Figure 19. Failure Appearance of controlled and VOCs contaminated LED

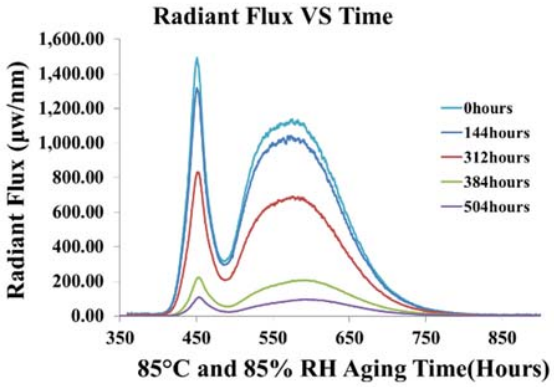

Figure 20. Radiant Flux Test Result of Group 1

The output spectrum of LED is predominately determined by two factors. The first is the semiconductor material that used to fabricate the chip. The second is the physical properties of the phosphor. Semiconductor material will determine the wavelength of the blue peak. The emitted wavelength of yellow peak is decided by the phosphor. For high power LEDs, the fabrication material usually is the InGaN which emits approximately450nm- 500nm blue light. In order to obtain white color spectrum, a portion of the blue light is absorbed by the phosphor and re-emitted from phosphor as yellow light. The physical properties of the chip and the phosphor can be monitored by recording the output spectrum of the LEDs. During the VOCs contamination, there is an obvious color change of phosphor. However, the discoloration is not caused by the change of physical or chemical properties of the phosphor. From the recorded radiant flux of Group 1 samples, there is no observable shift of the yellow peak in the emitted light. Once the black area on the phosphor is caused by the discoloration of VOCs, the discolored VOCs start to absorb emitted light. The absorption of the emitted light causes a degradation in the total luminous flux. Furthermore, during the absorption of light, the phosphor absorbed more blue light thus causing a shift in the chromaticity coordinates. Figure 20 shows the measured radiant flux of group 1 samples during the test.

Discoloration Analysis

In order to further study the contamination area of the LED package, a pair of control-group sample and contaminated sample were cross sectioned from the middle area where the discoloration had been observed in the contaminated set samples (the red line used for the cross-section is shown in Figure 21). Figure 21 shows the middle line and polished surface images of the LED package.

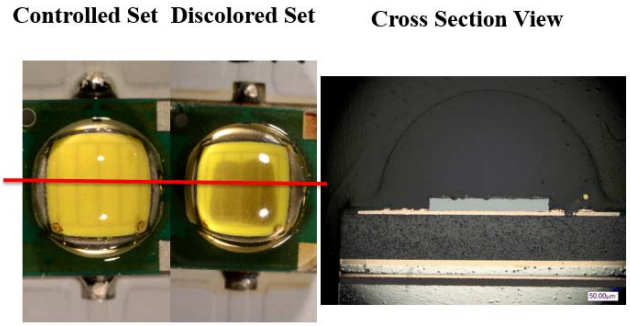

Figure 21. Cross Sectioned LED Package

Detailed analysis were performed on the area near the LED chip in the package. It is important to understand the architecture of the chip before analysis. Different architectures of LED chip have been used in commercial products to increase the photon extraction efficiency and to maximize the power output. The samples used in this experiment had a vertical layout and also called vertical LED (VLED). During the fabrication, the laser liftoff (LLO) and chemical lift off methods are utilized to separate LED epitaxial layer from the sapphire substrate, because of its poor heat conductivity. The epitaxial layer were then transferred to electrically and thermally conducting silicon supporters. Figure 22 shows the magnified view of the chip area. From the image, different layers can be seen clearly.

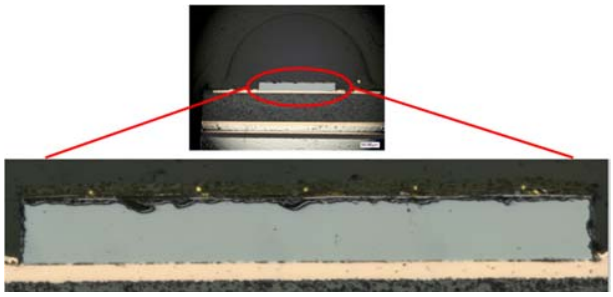

Figure 22. Chip Area View of LED Package

Because of its unique vertical architecture, the LED chip is actually a combination of several different layers. In this paper, 5 layers were identified to help understanding the place where VOCs contamination happened. In the following Figure 23. The five-layers have been marked for further analysis. Each of them are the potential location where discoloration happens. A schematic diagram is shown in Figure 23 to identify each layer in the vertical structure of LED chip.

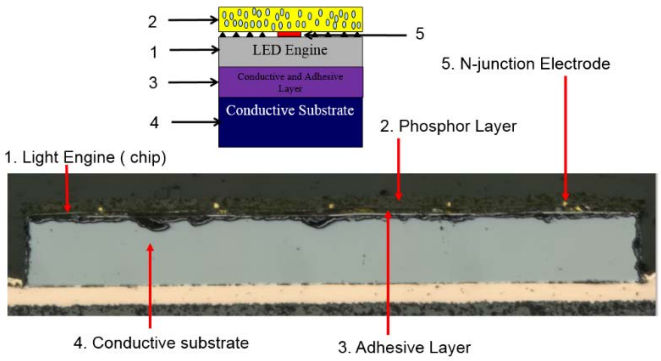

Figure 23. Layers of LED Chip

SEM image of the chip area were taken to further identify the epitaxial layer area. The rectangular in Figure 24 shows the epitaxial layer. From the image, surface pattern and n-electrode can be observed very clearly. The thickness of the thin film chip is about 2-3 µm.

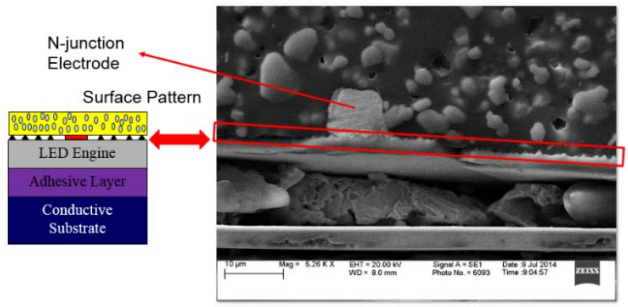

Figure 24. SEM View of the Chip Area

Optical images of high magnification were taken in both the control-group and the contaminated samples to observe how and where the VOC contamination happened. Figure 25 shows the comparison between the controlled sample and contaminated samples at the chip-phosphor layer interface. There is an obvious color change in both the phosphor layer and the adhesive layer. From the VOCs contamination theory, the contamination should only happens in phosphor binder layer. In the next analysis phase, a detailed analysis were performed on the adhesive layer with SEM (Scanning electron Microscopy) and EDX (Energy-dispersive X-ray) technology to explain the reason for discolored adhesive layer.

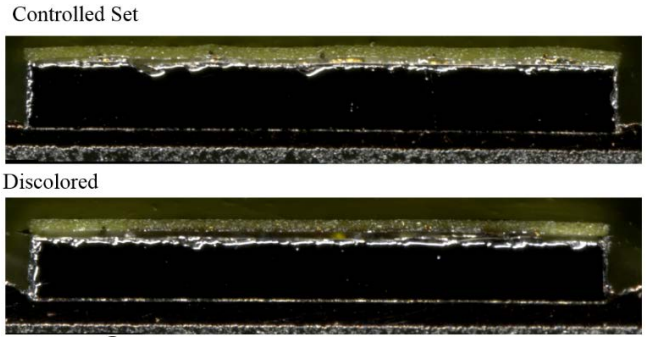

Figure 25. Optical Image Comparison of LED Chip

During the analysis of the adhesive layer, SEM image were taken and EDX analysis were performed to decide what had changed in this layer. EDX spectroscopy (EDS, EDX, or XEDS), which also called energy dispersive X-ray analysis is an elemental analysis technique which can tell the composition of each element. The following Figure 26 shows the SEM pictures and EDX analysis of the adhesive layer:

Element	Weight %	Atomic%
B K	4.42	25.04
C K	6.38	32.54
N K	2.94	12.84
Al K	0.71	1.62
Ga K	2.39	2.10
Au M	83.15	25.85
Totals	100.00	

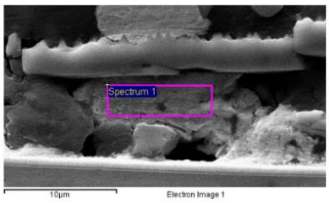

Figure 26. SEM View and EDX Analysis of Adhesive and Conductive Layer

From the test result, gold is the main component of the adhesive layer and this element is very stable. There are supposed to be no change of that layer. Also, the following Figure 27 shows that the adhesive layer is not continuous and most part of the layer is empty which make sense considering the high cost of gold. In conclusion, the adhesive layer is impossible contaminated by the VOCs and it is becoming black is caused by optic illusion. The light engine and silicon binder are both transparent. When light goes inside of the empty space of the adhesive layer, it will be reflected out by the mirror layer. However, when the phosphor layer was contaminated by VOCs and become black. The light goes inside of the empty space of adhesive layer will be absorbed by phosphor layer which makes the adhesive layer looks black. Actually, it is just optical illusion.

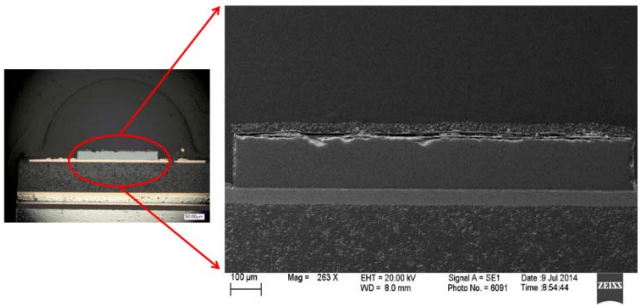

Figure 27. SEM View of the Whole Chip Area

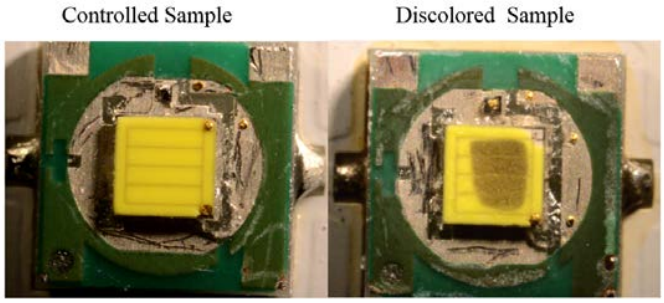

Figure 28. Comparison of Removed Lens Samples

In conclusion, the contamination area only appears in the phosphor layer. This conclusion can also be proved by the comparison between the controlled sample and the discolored sample, when their lens are removed. Figure 28 shows the comparison. It is obvious from the figure that only the phosphor layer become black.

Summary and Conclusions

Experimental data presented in the paper shows that vulcanized rubbers and adhesive epoxies operating in high temperature and high humidity environments in the vicinity of the LED-based product may give off VOCs and affect the luminous flux output and color stability of the product dramatically and pre-maturely. Furthermore, since rubbers and epoxies may be used in the construction of the LEDs, Solid State Luminaires – given the drastic impact of the VOC outgassing on the LED performance and reliability shown by the data in this paper, it is imperative that examination of the interactions of the material composition with the luminous flux output and color shift of the LED be examined for critical applications. Temperature humidity exposure has been shown in this paper to be a quick and effective way to test the interaction between the outgassing of rubbers and epoxies on the luminous flux output and color shift. While epoxies and glues in LED applications may be conventionally chosen for heat management, accommodating the thermal mismatch and maintaining good adhesion over the lifetime of the LED and SSL – the requirement for adequate lifetime without significant luminous flux degradation and color shift will necessitate that the materials be thermally stable without significant outgassing while operating at high temperature and high humidity.

Acknowledgments

The work presented here in this paper has been supported by a research grant from the Department of Energy under Award Number DE-EE0005124.

References

Cree XLamp LEDsChemical Compatibility, Cree, Inc., Durham, NC. , CLD-AP63 rev 4 August, 2013.

Damann M, Leuther A, Benkhelifa F, Feltgen T, Jantz W. Reliability and degradation mechanism of AlGaAs/InGaAs and InAlAs/InGaAs HEMTs. Physical status solid: Basic research, Volume 195, Issue 1, Pages, 81–86, January 2003.

Davis, J.L., K. Mills, M. Lamvik, R. Yaga, S.D. Shepherd, J. Bittle, N. Baldasaro, E. Solano, G. Bobashev, C. Johnson, and A. Mills. 2014. System reliability for LED–based products. In Proceedings of the 2014 15th International Conference on Thermal, Mechanical, and Multi-physics Simulation and Experiments in Microelectronics and Microsystems (IEEE EuroSimE), Ghent, Belgium. April.

Davis, J.L., M. Lamvik, J. Bittle, S. Shepherd, R. Yaga, N. Baldasaro, E. Solano, and G. Bobashev. 2013. Insights into accelerated aging of SSL luminaires. Pp. 88350L-1–88350L-10 in Proceedings of SPIE 8835: LED-based Illumination Systems, San Diego, CA.

Deane B.Judd, Estimation of Chromaticity Difference and Nearest Color Temperature on the Standard 1931 ICI Colorimetric Coordinate System, National Bureau of Standards Washington, D.C., 1936

Electrical and Photometric Measurements of Solid-State Lighting Products, IES-LM-79-08, 2008.

Fujii, T., Y. Gao, R. Sharma, E. L. Hu, S. P. DenBaars and S. Nakamura, Increase in the extraction efficiency of GaN-based light-emitting diodes via surface roughening, Appl. Phys. Lett. 84, 855 (2004)

Gernot Hoffmann, Graphics for Color Science, 2004

Hoang T, LeMinh P, Holleman J, Schmitz J. The effect of dislocation loops on the light emission of silicon LEDs. 35th European solid-state device research conference; Pages 359–362, 2005.

Hong Luo, Jong Kyu Kim, E. Fred Schubert, Analysis of high-power packages for phosphor-based white-light-emitting diodes. Appl. Phys. Lett. 86, 243505 (2005)

Hyunsoo Kim, Kyoung-Kook Kim, Kwang-Ki Choi, Hyungkun Kim, June-O Song, Jaehee Cho, Kwang HyeonBaik, Cheolsoo Sone, Yongjo Park, and Tae-Yeon Seong, Design of high-efficiency GaN-based light emitting diodes with vertical injection geometry, Appl. Phys. Lett. 91, 023510 (2007).

JEDEC Steady State Temperature Humidity Bias Life Test Standard, JESD22-A101C, 2009.

Koh, van Driel, and Zhang. Degradation of epoxy lens materials in LED systems. 2011 12th International Conference of Thermal, Mechanical and Multiphysics Simulation and Experiments in Microelectronics and Microsystems (EuroSimE 2011) 1/5 - 5/5.

Lee, S.-N., Paek, H. S., Son, J. K., Kim, H., Kim, K. K., Ha, K. H., Nam, O. H. and Park, Y., "Effects of Mg dopant on the degradation of InGaN multiple quantum wells in AlInGaN-based light emitting devices", Journal of Electroceramics 10.1007/s10832-008-9478-2 (2008)

Meneghesso G, Leveda S, Zanoni E, Scamarcio G, Mura G, Podda S, et al. Reliability of visible GaN LEDs in plastic package. Microelectronics Reliability, Volume 43, Issues 9–11, Pages 1737–1742, September–November 2003.

Moon-Hwan Chang , Diganta Das, P.V. Varde ,Michael Pecht , Light emitting diodes reliability review, Microelectronics Reliability, Volume 52, Issue 5, Pages 762–782, 2012.

N. Narendran*, Y. Gu, J.P. Freyssinier, H. Yu, L. Deng, Solid-state lighting failure analysis of white LEDs, Journal of Crystal Growth, Volume 268, Issues 3–4, Pages 449–456, 1 August 2004.

Pavesi M, Manfredi M, Salviati G, Armani N, Rossi F, Meneghesso G, et al. Optical evidence of an electrothermal degradation of InGaN-based light-emitting diodes during electrical stress. Appl. Phys. Lett. 84, 3403 (2004).

Rossi, F., Pavesi, M., Meneghini, M., Salviati, G"Influence of short-term low current dc aging on the electrical and optical properties of InGaN blue light-emitting diodes", J. Appl. Phys. 99, 053104-1-053104-7 (2006)

SAMSUNG Chemical guide of LED Component, SAMSUNG Inc., 2013

Schanda, J., Colorimetry: Understanding the CIE System. Hoboken, NJ, USA: Wiley, 2007.

Schubert, E. F., Light-Emitting Diodes, 2nd ed. Cambridge: Cambridge University Press, 2006.

Specifications for the Chromaticity of Solid State Lighting Products: For Electric Lamps, ANSI_ANSLG C78.377-2011, 2011, National Electrical Manufacturers

Association/American National Standard Lighting Group, Rosslyn, VA, USA.

Tomiya, S., Hino, T., Goto, S., Takeya, M., and Ikeda, M., "Dislocation related issues in the degradation of GaNbased laser diodes," IEEE Journal of Selected Topics in Quantum Electronics 10, 1277-1286 (2004)

Ye, S., F. Xiao, Y. X. Pan, Y. Y. Ma, and Q. Y. Zhang, "Phosphors in phosphor-converted white light emitting diodes: Recent advances in materials, techniques and properties," Mater. Sci. Eng. R, Rep., vol. 71, no. 1, pp. 1–34, Dec. 2010.

Zhang Qin, Jiao Feng ,Effect of temperature and moisture on the luminescence properties of silicone filled with YAG phosphor, Journal of Semiconductors , Vol. 32, No. 1,page 1-3,January 2011